Chapter 2

ENERGY ANALYSIS IN FIELD ION MICROSCOPY.

2.1 Introduction.

Energy analysis of field-ionized gas atoms is one of the few techniques available to test the accuracy of theories about field-ion image formation. To see how this is so, consider fig. (2.1). This diagram shows the electron potential energy for an atom in the high electric field near a field-ion specimen. In free space (a) the atom may be ionized by the electron tunnelling from the bound level through the reduced barrier provided by the field (Oppenheimer 1928). There is an extra constraint close to the surface (b): the electron now tunnels from the atom into the metal and must be received into an empty energy level (Inghram and Gomer 1954). Such levels are only available above the Fermi level, and so there exists a critical distance from the surface, x_c, within which it is not possible for ionization of the atom to occur. This distance is dependent on the ionization potential of the atom, I, and on the field. Once ionization has occurred, the ion formed gains energy from the field and the total energy available to it depends on the electrical potential of the point at which it was formed; measurement of the ion's final energy therefore indicates its place of origin. Considerations of the tunnelling probability as a function of field, and of the gas supply to the surface (Southon 1963), show that the ions will be formed mainly close to the critical distance at moderate fields, and the energy distribution will be as shown schematically (c).

2.2 Previous Work on Energy Analysis.

Inghram and Gomer (1954) used a magnetic spectrometer to show that the energy distribution of the field-ions was less than 20 eV wide; later, Muller and Bahadur (1956) used a simple retarding analyser to show the existance of the critical distance x_c and the narrow half-width of the distribution from argon, which was still less than the 2 eV resolution of their analyser. Tsong and Muller (1964) extended the available data to neon and helium, using an improved analyser. Boudreaux and Cutler (1965, 1966) calculated the half-width of the ionization zone for hydrogen, using a variety of quantum-mechanical approaches, and found that at a field of 2.3 volts/Angstrom unit the zone should be about 0.12 A wide, corresponding to an energy distribution half-width of 0.27 volts.

Jason (1965) measured multiple peaks in the energy distributions of hydrogen and neon which (1966, 1967) were interpreted as due to Bohr-type standing waves between the metal surface and the potential of the applied field. Alferieff and Duke (1967) considered that the effect was due to interference between waves reflected from the metal surface and the potential of the atom concerned. Yet a further interpretation has come from Lucas (1971) who considered that the sudden formation and subsequent rapid acceleration of the gas ions should excite surface plasmons in the metal: the discrete energy peaks are then due to the loss of integral numbers of energy quanta to the surface plasmons.

Utsumi (1973) has measured the detailed energy spectra of hydrogen, neon and helium ionized above tungsten and platinum emitters, in an attempt to distinguish between the various alternative quantum-mechanical models of the ionization process which have been published. These include the 1D WKB method

(Tsong and Muller 1964), the rearrangement-collision Born approximation and metal plane-wave/atomic plane-wave methods of Boudreaux and Cutler (1966 a,b), the 6s,5d metal orbitals/atomic wave interaction method of Iwasaki and Nakamura (1972), and the Bardeen-type transfer Hamiltonian method of Appelbaum (1973). No firm experimental distinction between the methods has yet appeared.

In Jason's 1967 paper the energy spectrum of neon which was presented showed signs of ionization at higher energies than those of the main peak of the distribution; that is, ions were apparently formed closer to the tip than the critical distance. Krshnaswamy and Muller (1973), using a Mollenstadt analyser, also found Jason peaks in the energy spectra of helium and neon and claimed that ions could be formed in the forbidden region in mixtures of neon or helium and hydrogen, due to electron-impact ionization, or desorption of electron-impact excited, field-adsorbed inert gas by the electron shower from the hydrogen ionizing far from the surface. As the cross-section for such processes was thought to be low, and as it is possible for misaligned Mollenstadt analysers to produce 'ghost' spectral lines, there was some small doubt about this latter result.

2.3 Energy Analysis and Field Evaporation.

As outlined in Chapter 1, the atom-probe is a combination of a field-ion microscope and a time-of-flight mass spectrometer. Ions are evaporated from a metal surface using a short high-voltage pulse, and their flight-time t to a detector a distance L away is measured. As the energy of the ions is given by the sum of the

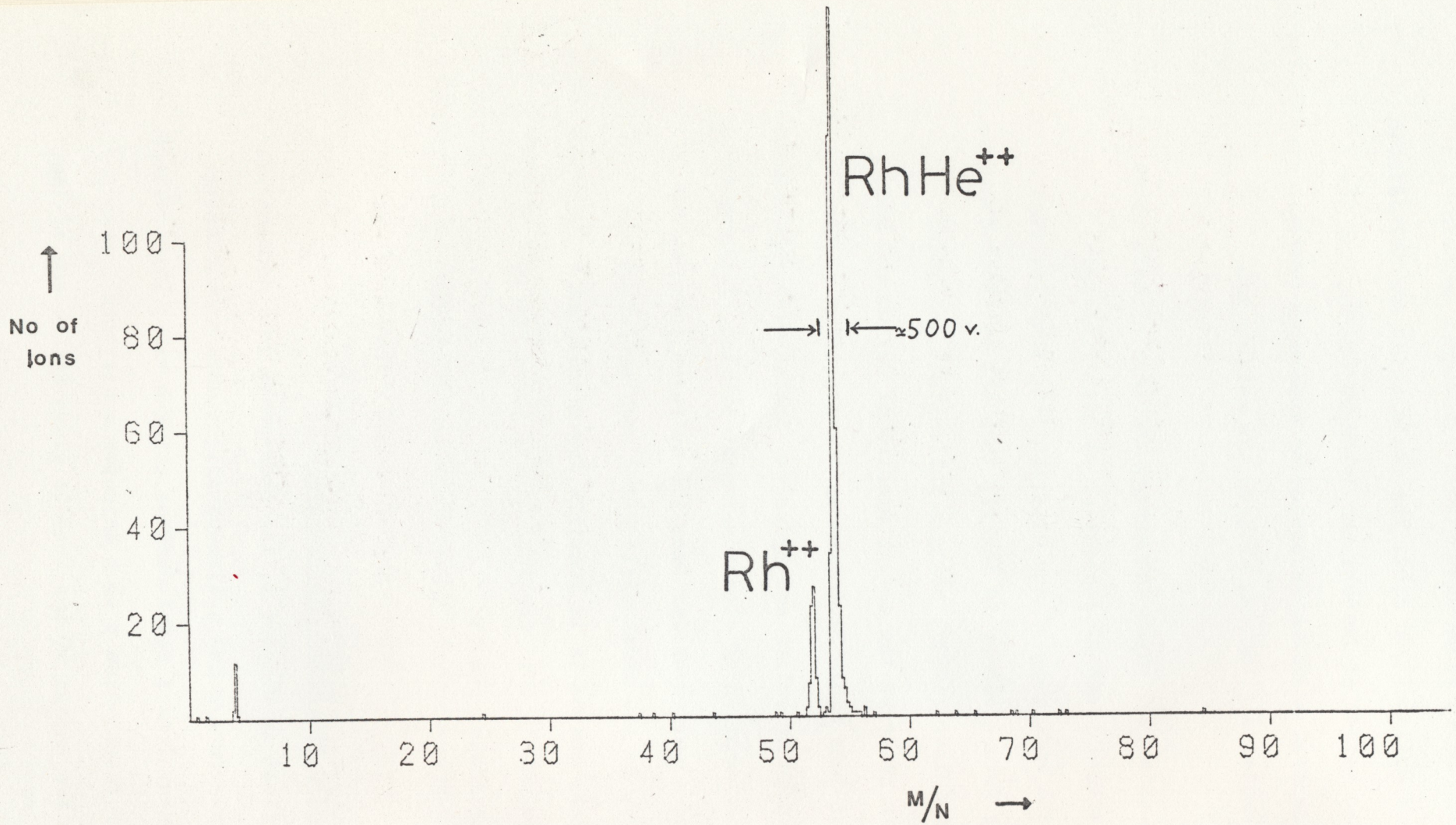
No of Ions
100
80
60
40
20
RhHe++
≃500 v.
Rh++
10
20
30
40
50
60
70
80
90
100
M/N

Fig. 2.2

specimen standing voltage V and the pulse voltage P, the mass to charge ratio of the ions may be easily calculated;

$$\tfrac{1}{2} m v^2 = n e (V + P)$$

$$\& \qquad v = L/t$$

$$\text{so} \qquad m/ne = 2 (V + P) t^2/L^2$$

The atom-probe has been used to provide useful metallurgical information, for example in the analysis of small precipitate particles(Brenner and Goodman 1971, Turner, Regan and Southon 1972).

The mass-resolution of the atom-probe becomes important in the analysis of systems in which ions of similar mass to charge ratio may be formed; for example, in systems where hydrides of heavy metals are formed, and in alloy steels, where a large number of elements are present, each with several abundant isotopes, poor resolution can cause difficulties in unravelling the mass-spectrum obtained. The situation is worsened by the fact that the mass-peaks of monoisotopic elements are found to have a finite width. This is illustrated by fig (2.2), which is a mass-spectrum of rhodium in the presence of helium imaging gas. The presence of a rhodium-helium complex ion, previously reported by Muller et al (1969), is clearly shown; both the Rh^{++} and $RhHe^{++}$ peaks are seen to have a considerable width.**

** The all-stainless steel UHV atom-probe used in this work was designed by Dr P.J. Turner and has been described elsewhere (Turner et al 1972). Flight times were measured using a 100 MHz digital timer designed and built by Dr B.J. Regan (Regan 1973). The assistance of Dr Turner in operating the atom probe for this work is gratefully acknowledged.

The finite width of the mass peaks shown is not due to errors in measuring flight-times which are measured extremely accurately. It is apparently due to a spread in the energies of the ions evaporated from the specimen, and an appropriate energy scale for the Rh^{++} and $RhHe^{++}$ peaks is shown in fig (2.2). Various suggestions have been made as to how the energy spread arises. These include premature evaporation of the ions before the maximum pulse voltage has been reached (Krishnaswamy and Muller 1973), to ions still being in the field of the tip when the pulse voltage starts to decay (Regan 1973) and in special cases to the breakup of complex ions.

The first of these reasons is probably appropriate when large evaporation pulses are applied to a specimen in the presence of an image gas. Muller commonly uses such pulses in the search for rare charge species but, as has been pointed out elsewhere (Turner Regan and Southon 1972), high evaporation rates are not suitable in quantitative metallurgical applications, where low rates must be employed in order to prevent several ions arriving simultaneously at the detector and being counted only as one ion. At low evaporation rates the energy spread is probably due to ions 'seeing' the falling edge of the evaporation pulse, and calculations (Regan 1973) have shown this to be likely.
A further source of energy losses has been suggested by Lucas (1971) who suggested that the departing metal ion might lose energy to surface plasmons, in the same way as he had predicted for image gas ions. The energy losses predicted were quite large: for tungsten, N surface plasmons, of energy 7 eV, would be excited by the evaporation of an ion of charge ne, where N has a Poisson distribution of mean

$N_m = 4\ n^2$; for W^{3+}, $N_m = 36$, so the mean energy loss would be 252 eV, corresponding to a change in specimen voltage of 84 volts. Regan (1973) has pointed out that the uncertainty in this deficit is given by the standard deviation of the Poisson distribution, giving an uncertainty of $7 \times 2n = 42$ eV, corresponding to 14 volts. The net result is a narrow mass peak with a mass shift of $28\ n\ M\ V^{-1}$, where M is the mass and V the tip voltage. Muller and Tsong (1973) state that the energy deficit of Ta^{3+} was greater than that of Ta^{4+}, and claimed that this proved that plasmon losses were not observed. However, the predicted mass shift and peak broadening are sufficiently small that they would have been obscured by pulse-effects in this experiment, and their conclusion is not valid.

During the course of the present work Krishnaswamy and Muller (1973) described an atom-probe fitted with a 90° electrostatic energy analyser which they had used to show that a large energy spread does indeed exist for pulse-evaporated metal ions; they found that this spread is larger for ions of high mass/charge ratio, which was not unexpected, as the slower heavy ions are still in the vicinity of the specimen when the tip voltage starts to fall at the end of the pulse.

Lucas (1972) has produced further calculations showing that plasmon excitation by heavy metal ions was less likely than previously thought, due to the heavy metal ion being removed sufficiently slowly for any plasmon excitation to be adiabatically undone. However, he maintained his original theory that the 'Jason Peaks' in field-ionized gas spectra are due to plasmon losses. As these peaks have been observed for neon (m/n = 20.2) it does not seem clear that plasmon losses should not be expected

for metal ions of similar mass/charge ratio (e.g. Be^{+}, Al^{++} or Al^{+}, or even Fe^{++}). Further experiments on plasmon excitation are therefore seen to be desirable, to clarify the situation, and a suitable experimental technique for field-evaporated ions will be described below.

2.4 Current Work.

At the outset of this work there were several areas of energy analysis which seemed to merit further attention. These were a) A study of the fine details of energy spectra of field-ionized gases, to explore the influence of the band structure of the specimen on ion current and distribution, and the possibility of obtaining information on the electronic properties of the specimen surface (Knorr and Muller 1968, Iwasaki and Nakamura 1972) b) An extension of Jason's excellent work to mixtures of gases, to investigate the effect of field-adsorption on the energy spectrum. c) An investigation of the energies of field-evaporated ions, particularly with reference to the broadening of peaks in the atom-probe mass spectra, and the Lucas theory of energy loss to surface plasmons.

During the course of this work various other workers have published results which have modified the emphasis of the work described here. Utsumi (1973) has reported some results on the fine structure of energy distributions. Krishnaswamy and Muller (1973) reported the effect of hydrogen on field-adsorbed helium and neon, though their results were subject to some doubt for the reasons outlined above. Muller and Krishnaswamy (1973) described measurements of the energy-losses of pulse-field-evaporated metal

ions showing that the broad energy distribution expected from atom-probe spectra existed. Poschenrieder and Oetjen (1972) have described an energy compensated time-of-flight mass spectrometer capable of accurately mass-analysing ions even though they have a large energy spread; Krishnaswamy and Muller (1974) have described a copy of Poschenrieder's instrument which seems to work well as an atom-probe. The development of this device makes the energy spread of evaporated ions of less practical importance, but the energy distribution of metal ions, excluding pulse effects, is still of theoretical importance as will be shown below.

For these reasons, and for experimental reasons outlined below, only a limited amount of work on field ionization will be described in this thesis; in particular, evidence supporting the electron-impact desorption of adsorbed gases, described above, will be presented. Some results on the pulsed-evaporation of metal ions will be discussed, and in addition a technique for measuring accurately, for the first time, the energies of metal ions evaporated under effectively steady-field conditions will be described.A comparison of the experimental results with existing theories of field-evaporation emphasises the inadequacies of such theories.

2.5.1 The Selection of a Suitable Spectrometer.

The design of a spectrometer suitable for energy analysis of field-ionized gas ions and field-evaporated metal ions needs some care. A first consideration is that the spectrometer should select ions produced from a relatively small area of the specimen (say less than 5^{o} acceptance angle) so that the crystallographic nature of the surface from which the ions are taken is relatively well defined. This constraint has two effects; firstly,as many types of spectrometer can be operated at high energy-resolution only when the ion beam has a narrow cone-angle, it simplifies spectrometer design; secondly, as the number of ions available for analysis varies with the selected specimen area, and hence with the square of the cone-angle, too narrow a cone-angle will result in a very low ion flux and hence signal to noise ratio problems. The low ion fluxes available from a field-ion specimen make this particularly serious. The image-gas ion current available from each image-point is around 10^{3} ions/second at 10^{-5} Torr and best image voltage (BIV); below BIV the ion current falls very rapidly and depends on the 30^{th} power of the voltage (Southon 1963). The ion current is proportional to pressure, but too high a pressure leads to problems with collisions between ions and neutral gas atoms (Forbes 1970). Differential pumping between the specimen and spectrometer (Jason 1967) may be used to reduce this problem, but even so the ion current from a small area is limited to around 10^{4}-10^{5} ions/second at most and will be significantly less at low fields. This in itself would not be particularly serious, as pulse-counting techniques and multi-channel scalers are frequently used in other types of experiment to build up a

spectrum from much lower currents, over periods of minutes. The special nature of the field-ion source makes this difficult if not impossible; if the emitting area consists of only a few surface atoms, the specimen must be completely stable against field-evaporation or etching during the course of the experiment. Furthermore, vacuum requirements become extremely stringent. This may be illustrated by the fact that if a partial pressure of $1\ 10^{-8}$ Torr of neon is present when a tungsten specimen is imaged in helium at $78^{\circ}K$, 'bright spots' are seen to appear and disappear on the surface, with residence times typically between 0.1 and 1 second (Schmidt, Reisner, and Krautz 1971); these spots correspond to the field-adsorption and desorption of neon atoms. At low temperatures the residence times of the neon atoms becomes very much longer ($t \propto e^{Q_{ads}/kT}$) and a more complete coverage of the surface will result. Since the adsorbed neon is only visible because of the considerable effect it has in enhancing the local ion current, it may also be expected to influence any fine details in the energy spectrum, such as those expected as a result of the influence of the metal band-structure on field-ionization (Fonash and Schrenk 1969). Ultra-high vacuum techniques now available do considerably reduce the possibility of specimen contamination by hydrogen and water vapour from the residual gases in the system (Boyes 1974) but care still has to be taken that contaminants are not introduced either with an imaging gas or as a result of outgassing from some source, such as a channel-plate (van Oostrom 1969, Morgan 1970, Lewis and Gomer 1970) during the course of an experiment. Unless a spectrum can be taken rapidly (in a few seconds) so that changes in the condition of the specimen are apparent and can be eliminated, any claimed fine detail (on a scale of less than 1 volt) must be treated

with suspicion.

Measurements of the energy of field-evaporated ions puts even greater constraints on the type of spectrometer which may be used. The total number of metal ions which are available from a small area of the specimen surface may only be a few hundreds, before the specimen fractures or becomes too blunt. If a reasonably accurate energy distribution is to be obtained, every ion's energy must be measured and recorded. As the energy of the ions cannot of course be predicted exactly, all ions in a suitably wide range of energies must be detected and recorded simultaneously.

Three main types of spectrometer are available for measurement of ion energies: retarding-field analysers, dispersive analysers, and time-of-flight analysers. Retarding analysers have been used in previous measurements of field-ionized gas ion spectra, such as the work by Muller and Tsong referred to above. In these instruments a retarding electrostatic field is used to prevent ions reaching a detector, except those with sufficiently high enery. If there are $N(E)dE$ ions of energy between E and E+ dE per second, and the potential of the retarding electrode is V, the current reaching the detector is

$$i = \int_V^\infty N(E)\, dE$$

and after a time t the energy spectrum $N(E)$, obtained by differentiating the collector current with respect to V, is only known to an accuracy

$$\frac{\left(t \int_V^\infty N(E)\, dE \right)^{\frac{1}{2}}}{t \int_V^{V+\Delta V} N(E)\, dE}$$

as random current fluctuations in the high energy ion current obscure the small current due to ions with energy in the range V to V + ΔV. Long measurement times, of order minutes to hours, are mandatory if accurate energy spectra are to be obtained over a wide energy range. The advantage of the retarding analysers is that an absolute value of the ion energy is obtained from the retarding voltage. Staib (1972) has recently described a retarding analyser in which the higher-energy ions which have passed through the retarding barrier are focussed away from the detector, so that only ions with just sufficient energy to pass the barrier are detected: this allows measurement times to be greatly reduced. Such an analyser combines the better features of retarding analysers and differential analysers, to be described below, and could be usefully employed in future work on field-ionization.

Time of flight spectrometers include quadrupole spectrometers, in which ions of a particular mass and energy are selected by an oscillating electric field. The energy resolution is relatively poor, and as with the other time-of-flight spectrometer, both mass and energy contribute to any spectrum measured; they are not suitable for the present application.

The third class of spectrometer is that of the dispersive energy analysers. These include both electrostatic and magnetic types. Magnetic spectrometers use a shaped magnetic lens to deflect an ion beam and focus ions of a particular mass/charge ratio on a detector: as they actually focus ions of a particular

momentum, energy spectra can be obtained by a scan across a small mass range. The mass-sensitivity of a magnetic spectrometer can be useful in determining the identity of a particular ionic species, but also has disadvantages; as will be shown below, the known absolute energy of ions of one m/ne value may be used to determine the energy deficit of ions with another value, in an electrostatic spectrometer, but this is not possible in a magnetic spectrometer.

Electrostatic dispersive spectrometers use electrostatic fields to separate ions of differing energies independently of their mass. Plane, cylindrical, or spherical fields may be used to focus ions in an energy range E to E + ΔE onto a detector. The uncertainty in the measurement is now

$$\left\{ t \int_{E}^{E+\Delta E} N(E)\, dE \right\}^{\frac{1}{2}}$$

after a time t, and the time needed to scan a spectrum is greatly reduced from that needed for the retarding analyser. Against this advantage is that no absolute energy scale can be directly obtained. Kuyatt and Plummer (1972) have described a spherical consenser suitable for the measurement of the energies of field-emitted electrons; an excellent energy resolution of $\Delta E/E = 10^{-5}$ may be obtained with this spectrometer if careful machining and alignment procedures are followed. This spectrometer could be used in accurate measurements of field-ion energy distributions, but cannot analyse all energies simultaneously and so is not suitable for studying field-evaporated ions.

A solution to this problem is to use a dispersive spectrometer with a well-defined focal plane, at which a detector with spatial resolution and single-particle sensitivity may be placed. Cylindrical

Fig. 2.3 Parallel-Plate Energy Analyser.

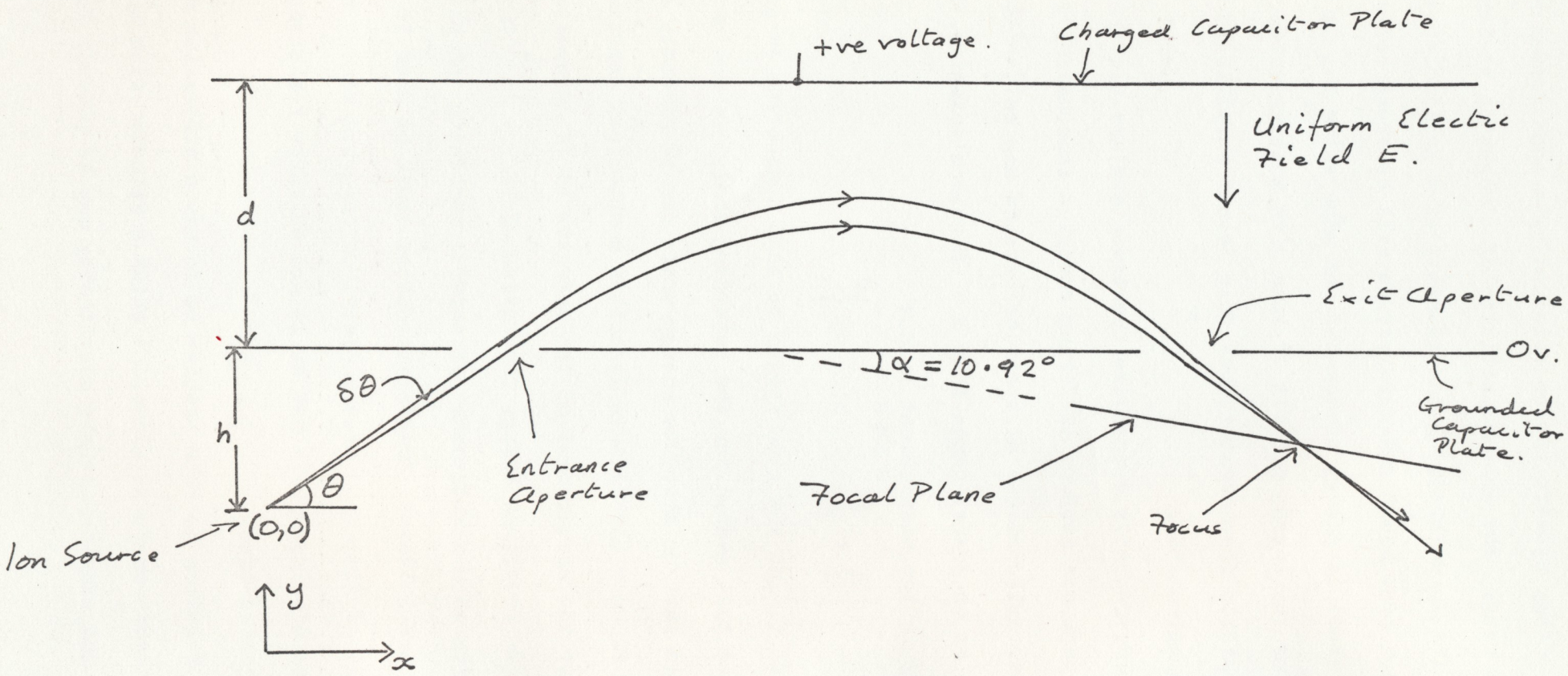

and parallel-plate spectrometers may be designed with suitable focal planes (which must, of course, be outside the focussing field if severe complications in detector design are to be avoided). Muller and Krishnaswamy (1973) have recently described a Mollenstadt analyser for use in field-ion microscopy; this device apparently has high resolution ($5\ 10^{-5}$) but no focussing action, so that an acceptance angle of less than $2.5\ 10^{-4}$ radians is necessary, thereby limiting the field-ion current to the unacceptably low value of 10-100 ions/second. The design of an alternative analyser using 90° electrostatic deflection was published during the course of this work (Krishnaswamy and Muller 1973) and would be a reasonable alternative to the instrument described below.

2.5.2 Parallel-Plate Spectrometers.

Parallel-plate spectrometers have been described in recent papers (Green and Proca 1970, Allen 1971) which are particularly suitable for focal plane detection. By using an entrance angle of 30° for the ion beam (fig (2.3)) both the source and the focal point of the beam are outside the spectrometer in a field-free region. This allows the use of a micro-channel plate intensifier as a focal-plane detector of the particles being analysed (Galanti, Gott and Renaud 1971). Following Green and Proca, the design of a spectrometer suitable for field-ion microscopy may be derived as follows.

Consider a source O, at a distance h from the spectometer, emitting a beam of particles of charge ne from a potential V, at an entrance angle θ to the spectrometer. Taking Cartesian coordinates x,y, the beam enters the spectrometer at

$x = h \cot \theta.$

Inside the spectrometer the equation of motion of the particles is given by

$$\frac{d^2y}{dt^2} = \frac{neE}{m} \qquad \frac{d^2x}{dt^2} = 0$$

where E is the electric field inside the spectrometer. Integrating, and taking t = 0 at the spectrometer entrance, we obtain

$$y = \frac{\frac{1}{2} n e E t^2}{m} - vt \sin \theta$$

so that y = 0 at t = 0 or $t = 2 m v \sin\theta/(neE)$.

$\frac{dx}{dt} = v \cos \theta$, so the particle leaves the spectrometer at

$$x = h \cot\theta + \frac{2 m v^2 \sin\theta \cos\theta}{n e E}$$

Substituting $\frac{1}{2} m v^2 = neV$, the trajectory of the ion outside the spectrometer is given by

$$x = (h + y) \cot \theta + 2 V/E \sin 2\theta \qquad (1)$$

We require the locus of the focal points of the spectrometer.

i.e. $$\left(\frac{dx}{d\theta}\right)_y = 0 = (h + y) \operatorname{cosec}^2\theta - \frac{4V}{E} \cos 2\theta$$

or $$h + y = \frac{4V}{E} \cos 2\theta \sin^2\theta \qquad (2)$$

Eliminating V, the focal line is given by

$$x = (h + y) \cot \theta + \tfrac{1}{2} (h + y) \frac{\sin^2\theta}{\cos 2\theta \sin^2\theta}$$

Rearranging, we obtain

$$y = \frac{\cos 2\theta \tan \theta}{1 + \cos 2\theta} - h ,$$

so that the focal plane is flat, and at an angle to the spectrometer plates of

$$\tan^{-1}\left(\frac{\cos 2\theta \tan \theta}{1 + \cos 2\theta} \right)$$

The value of θ at which aberrations of the spectrometer are a minimum is obtained by the following expansion:-

$$\Delta x = \Delta\theta \frac{dx}{d\theta} + \frac{(\Delta\theta)^2}{2} \frac{d^2x}{d\theta^2} + \frac{(\Delta\theta)^3}{6} \frac{d^3x}{d\theta^3} + \ldots$$

$$= \frac{2V}{E} \left(\frac{2\Delta\theta^2 \cos 3\theta}{\sin \theta} - \frac{2}{3} \left(\frac{3 \sin 3\theta \sin\theta + \cos 3\theta \cos\theta}{\sin^2\theta} \right) \Delta\theta^3 + \ldots \right)$$

For $\theta = 30^\circ$ the term in $\Delta\theta^2$ is zero and we have second order focussing, with

$$\Delta x = - \frac{8V}{E} \Delta\theta^3 \qquad (3)$$

as the change in x for an angular increment of $\Delta\theta$.

For $\theta = 30^\circ$, from equations (1) and (2) above we have

$$x = (h + y)\sqrt{3} + \frac{2V}{E} \cdot \frac{\sqrt{3}}{2}$$

and $$h + y = \frac{V}{2E}$$

so $$x = \frac{3V\sqrt{3}}{2E} \quad \text{and} \quad y = \frac{V}{2E} - h \text{ on the focal line} \qquad (4)$$

and $$\alpha = \tan^{-1} \frac{1}{3\sqrt{3}} = 10.92^\circ \qquad (5)$$

The dispersion of the spectrometer, that is, the distance along the focal plane by which the focus moves for a small increment in V, is given by

$$\ell^2 = (x_1 - x)^2 + (y_1 - y)^2 = \frac{28}{4E^2} \Delta V^2$$

or dispersion $D = \frac{\ell}{\Delta V} = \frac{\sqrt{7}}{E}$ (6)

so that there is a linear relation between position and energy.

2.5.3 Mechanical Size of Spectrometer.

The design of a practical parallel-plate spectrometer is governed by various considerations, including the total ion energy, the energy spread, the resolution required, the mechanical size of the source, and the linear resolution of the detector. For the field-evaporated ions the energy and energy spread were expected to be 5-15 KV and 200-500 V respectively, from the atom-probe spectra shown above. The resolution required for a useful study of field-ion energy spectra is of the order of 1 volt, or better. The linear resolution of a proximity-focussed channel-plate detector is typically of the order of 10 line-pairs/mm. Magnetically focussed channel-plate intensifiers (Turner et al 1969) have somewhat higher resolution, but the presence of a large magnetic field close to the spectrometer was felt to be undesirable. Proximity-focussed chevron channel-plates (Bendix Corp.) have the advantage of very high gain, and can be used for the detection of single ions (Brenner and McKinney 1972) but according to the manufacturers have a resolution of only 4 lp/mm.

Taking 10 lp/mm as the detector resolution, for a spectrometer to resolve 1 volt gives a dispersion D = 0.1 mm/volt = $\sqrt{7}/E$ or E = 26.4 volts/mm as the spectrometer field. For a 50 mm diameter channel-plate the width of the spectrum would be 500 volts.

The total ion energy at which this could be attained depends on the physical size of the instrument, and the width $\Delta\theta$ of the beam which is to be accepted. The maximum ion energy V_{max} which will arrive at the detector without intercepting the charged condenser plate is given by

$$E\,d = V_{max}\sin^2(30 + \Delta\theta)$$

where d is the spacing of the condenser plates. Taking d = 70 mm, which is a convenient size,

$x_{max} = \frac{3\sqrt{3}}{2E} V_{max}$ = 610 mm, for the field calculated above, and for $\Delta\theta = 3^\circ$.

Taking $x \; x_{max}$ = 550 mm, say,

$$V = \frac{2.550\,E}{3\sqrt{3}} = 5{,}6 \text{ KV for } E = 26{,}4 \text{ V/mm}.$$

We therefore expect the detector to be good enough to resolve 1 volt at a total energy of 5,6 KV, with a 500 volt energy window. Is this compatible with the energy resolution of the analyser itself?

From (3) above, $\Delta x = \frac{8\,V}{E}\Delta\theta^3$.

This corresponds to an energy spread on the detector of

$$\Delta V = \Delta x \sec\alpha\, D = 16/3\sqrt{3}\; V\Delta\theta^3$$

or $$\frac{\Delta V}{V} = 3.1\Delta\theta^3.$$

Green and Proca quote $\Delta V/V$ as $1.6\Delta\theta^3$: although they do not explicitly state it, this presumably takes into account the shape of the spectral line obtained from a uniform beam;

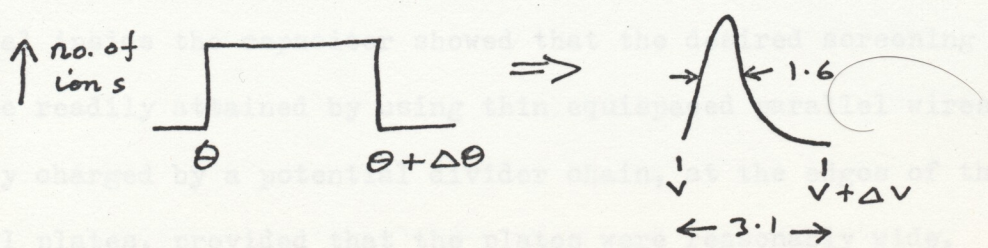

For $\Delta\theta = 3^{\circ}$, $\Delta V/V = 1.6\Delta\theta^3 = 2{,}3\cdot10^{-4}$.

For V = 5,6 KV, ΔV = 1,3 volts.

We therefore see that our initial selection of dimensions is not far wrong, and a very small reduction in $\Delta\theta$ will give the required 1 volt resolution, at the lower end of the total energy range required. This resolution is obtained at a beam cone-angle of 30°. Furthermore, no lenses are needed for this system, so there is no danger of artefact peaks in the spectrum due to chromatic lens aberrations, at the large spread in ion energies which can be simultaneously accepted and measured.

The spacing between the condenser and the detector may now be calculated. From equation (4)

$$y = V/2E - h = 106 - h$$

or $$y + h = 106 \text{ mm}.$$

Therefore, as y must not be negative, $h < 106$ mm, and h = 50 mm was taken as a convenient distance between the specimen and the earthed condenser plate.

2.5.4 Fringing Fields.

The analysis above assumes that the condenser plates extend to infinity in all directions, and that there is no disturbance of the field at the entrance and exit apertures of the spectrometer. In practice the spectrometer has to be confined within a small vacuum system and so the potential of surfaces outside the spectrometer must be screened by establishing equipotentials at the edges of the plates. A simple iterative calculation of the potential inside the capacitor showed that the desired screening could be readily attained by using thin equispaced parallel wires, suitably charged by a potential divider chain, at the edges of the parallel plates, provided that the plates were reasonably wide.

It had been anticipated (Green and Proca 1970) that the entrance and exit apertures of the spectrometer, which need to be large for ease of alignment as well as to provide the desired energy bandwidth of the detector, would need to be covered with wire mesh to establish the local fields. However, initial experiments without such meshes showed that the spectrometer could still be adjusted sufficiently well to provide the required resolution. The only effect of the fringing fields was to alter the curvature of the line focus obtained on the detector (the spectrometer, of course, only focusses the beam in one dimension). As this did not interfere with the use of the spectrometer, and as introducing meshes would have reduced the transmission efficiency of the analyser, and introduced a source of secondary electrons, they were not fitted to the spectrometer.

2.5.5 Mechanical Construction.

It was decided that the spectrometer should initially be built for use in a modest vacuum, and, if results justified it, that a more sophisticated version should be built from ultra-high vacuum compatible materials. Although the spectrometer performed well up to the theoretical predictions, considerations of time and expense prevented the construction of the UHV version, and the results presented here were obtained with the trial version.

The spectrometer plates have to be maintained flat, parallel, and insulated from one another over a working area of some 700x75 mm^2. They must also be non-magnetic. Aluminium alloy was chosen for the material of the trial design; flat glass plates with a conductive tin oxide or gold coating could perhaps be used for a bakeable version.The spectrometer plates were milled as flat as possible

Fig. 2.4

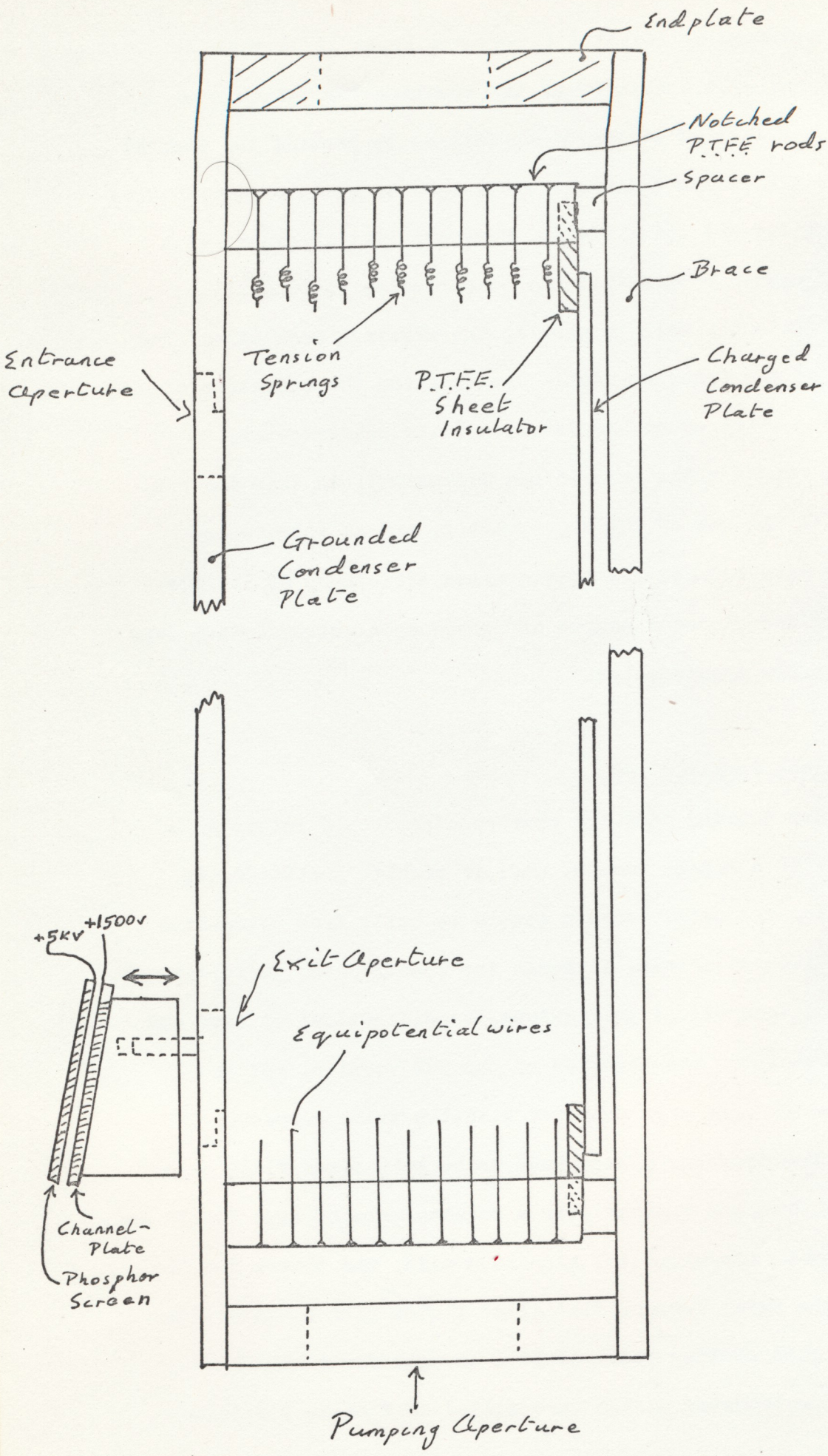
Endplate
Notched P.T.F.E. rods
Spacer
Brace
Entrance Aperture
Tension Springs
P.T.F.E. Sheet Insulator
Charged Condenser Plate
Grounded Condenser Plate
+5KV
+1500V
Exit Aperture
Equipotential wires
Channel-Plate
Phosphor Screen
Pumping Aperture

after bolting them down on a backing plate. Entrance and exit apertures were milled in the 12mm thick earthed plate: the surface adjacent to the apertures and outside the condenser was profiled so that the beam was not intercepted. The slight residual curvature in the grounded plate was removed using a parallel bar, outside the condenser, as a brace(fig (2.4)). This also supported, via a framework, PTFE insulators which held the charged plate in position.The equipotential wires were held in equispaced grooves machined 5 mm apart in four PTFE rods at the corners of the charged plate: the parallel ends of these rods also held the condenser plates parallel. The wires were 38 swg bare copper, and small stainless steel springs held each wire in tension. An internal chain of 13x 1M 5% resistors was used to supply the potential for the wires. The whole spectrometer was designed to be supported hanging vertically from one end, so that the plates would not sag.** Following this machining, the alloy parts of the spectrometer were cleaned by immersion in caustic soda solution, followed by a brief immersion in dilute nitric acid, to remove surface films of grease, etc. Charging of the oxide film on the plates did not appear to be a problem, and no attempt was made to modify their surface (i.e. by gold plating).

2.5.6 The Field Ion Source.

The field--ion specimen was supported on a manipulator system which allowed the ion beam to be aligned with the spectrometer

** My thanks go to Mr. D Starnell for machining parts for the spectrometer.

and which allowed some choice of the area on the specimen from which the ions were derived. This was achieved using a pair of concentric shafts sealed through the wall of the vacuum system using PTFE seals (Mills 1972). The specimen was supported on the inner shaft, and the field-ion microscope screen, with a 2 mm probehole, was carried on the outer shaft. The inner shaft could be rotated relative to the screen, to allow a 1-dimensional choice of emitting area; sliding this shaft in or out allowed the entrance angle of the beam to the spectrometer to be adjusted. Rotating the inner and outer shafts together allowed the beam to be steered in the transverse plane, and sliding them simultaneously allowed the position of the focal plane to be moved until it coincided with the plane of the detector. This was further facilitated by mounting the detector on a pair of rails attached to the earthed analyser plate, so that it could be moved perpendicular to the plates via a stainless steel bellows and an external screw. As this motion disturbed the focus of the camera system (see below) this operation was only used for initial alignment of the system.

The field-ion specimens were spot-welded onto 1mm diameter nickel tubes, which were then push-fitted onto a nickel pin which passed through a recrystallized alumina tube 3 mm in diameter overall; this tube served as the high-voltage insulation for the specimen. The alumina tube passed through a copper block, to which a heavy flexible copper braid was attached. The other end of the braid was bolted to a copper block brazed into the end of a 250 mm length of thin-walled stainless tubing, which served as a cryostat. The copper block carrying the specimen was a push-fit into a stainless-steel sleeve which served as a mantle around the specimen: this sleeve was attached to the inner rotating shaft of the manipulator

by a length of thin stainless steel strip, which provided some thermal insulation for the specimen. Judging by the quality and stability of the field-ion images which were obtained, the specimen temperature was very close to the temperature of the coolant in the cryostat. Liquid nitrogen and occasionally pumped nitrogen-oxygen eutectic were used as coolants.

The high voltage was carried to the specimen on a thin flexible molybdenum wire, routed so as to avoid deflecting the trajectory of the ion beam. The field-ion image was viewed directly from the specimen side of a layer of FF12 ZnS phosphor deposited on a tin-oxide coated glass disc, using a silicate binder. This screen was later modified and insulated, for reasons which will be described below.

2.5.7 The Detection System.

The feasibility of using this type of analyser to detect single ions relies on the availability of an extended detector with sufficient gain and sufficiently high spatial resolution and with sufficiently small background noise level. The microchannel-plate is now commonly used in field-ion microscopy to convert the image current of gas ions into an amplified electron current (Turner et al 1969). The microchannel plate is a closepacked array of semiconducting glass tubes, each approximately 1mm long and 40 um or less in diameter. A potential of order 1 KV is applied along the tubes, via a metal film deposited on the surface of the plate. Each incident ion creates a number of secondary electrons, and these are amplified by an avalanche process within the channel to produce an amplified output pulse of electrons at the far side of the plate. The gain of the plate is varied by varying the applied voltage, and may be as high as 10^5 at relatively high voltages

(1500 volts) (Mullard datasheet). It has been found that the size of the output pulse obeys an exponentially decreasing type of distribution at low applied voltages, but approaches a saturated type of distribution at high gains, with a rather more constant number of electrons produced by each incident ion (see Acta Electronica 14.2, 1971).

The output pulse of electrons must be recorded in such a manner that the position of the emitting channel is recorded. Various possibilities arise. The electrons could be used to expose a film directly, by using a high electrostatic field and a magnetic field to focus them onto a thin mica window separating the vacuum chamber and a nuclear emulsion outside the chamber; this mechanism is used in Spectracon image intensifiers (McGee et al 1969) and is very efficient, but is relatively cumbersome to construct and operate. A better solution is to proximity-focus the electrons onto a phosphor screen, using a high accelerating voltage (5 KV) and a small gap (1 mm), so that the resulting scintillation is small and bright. Using such a system it is possible to attain a resolution of 10 lp/mm (Turner 1967). The phosphor can be deposited on a fibre-optic plate, which serves as a vacuum window and couples the light from the phosphor onto a film held against its surface; the optical coupling is very efficient, and Galanti et al (1971), who used this system for the output from their parallel-plate spectrometer, were able to record individual ions. This system has the disadvantages that a) it requires a non-standard, and therefore expensive, fibre-optic window and b) the light output from the phosphor cannot be monitored visually when a photograph is being recorded.This is a serious problem when the spectrometer is being used to record transient spectra, such as those of pulse-evaporated ions.

The light output from the phosphor may most conveniently be recorded by using a plane glass window and a close-up lens system to couple the light onto standard 35 mm film. As lenses are very inefficient light-gatherers, compared to fibre-optics, it is important that wide-aperture optics are used. A very efficient way of collecting the light from a phosphor (Cartwright 1971) is to use two short-focus wide-aperture lenses front-to-front: the phosphor is at the focus of one lens , and the film is at the focus of the other. The light reaching the film is then of the order of 0,4 % of that emitted by the phosphor, using a Dallmeyer f1,9 lens as the first lens, and a Canon f,89 lens on the camera. The number of photons/ reaching the film for each incident ion may now be calculated as (gain of channel-plate)x(acceleration voltage)x(phosphor efficiency)x x(optical efficiency)/(photon energy)

$$= 10^4 \times 5000 \times 10^{-1} \times 4 \times 10^{-3} \times \tfrac{1}{4} = 5\ 10^3.$$

The demagnification of the lens system is approximately 2/5, so the number of photons per unit area of film is approximately $3\ 10^6$ photons/mm^2, which is marginally enough to cause a significant exposure of the film, according to the manufacturers data: the two fast films used in this study were Kodak Tri-X (nominally 400 ASA) and Kodak 2475 recording film (4000 ASA). The Tri-X was developed for 15 minutes in D 76 developer, diluted 1:1, at 20°C, to ensure maximum speed and contrast. The 2475 was developed in DK 50. Although 2475 is nominally faster than Tri-X, it has a much higher background noise level, and Tri-X was found to be very staisfactory for this work.

Tests made at low ion-current levels showed that individual ions could indeed be recorded on film, providing that the channel-plate was operated at high gain (operating voltage 1200-1500 volts). Even at the highest voltage possible there was still a fairly wide

variation in the density of the individual spots on the film, due to the lack of completely saturated channel-plate gain. It is felt that the major portion of the ions produced scintillations bright enough to be recorded, and the detection efficiency is estimated as (open area of channel-plate) x (recording efficiency)

$\simeq$ 65% x (say 80%) $\simeq$ 50%.

2.5.8 Noise Level.

Two sorts of channel-plate noise may be identified. Firstly, there are usually some permanently-emitting 'lit-up' channels, which appear in all photographs and may be eliminated by inspection. The channel-plate used in this analyser (Bendix 50 mm diam. x 40 μm channel) had only a small number of such channels at one time ($\lesssim$ 5). Secondly, there are random output pulses from channels; these are a rapidly increasing function of the applied voltage, and become prohibitively frequent at channel-plate voltages above about 1500 volts, except under pulsed conditions as will be described below (Chapter 7). By using suitable exposure times at any given channel-plate voltage and for any particular experiment, as detailed below, no insuperable problems with channel-plate noise were found.

2.5.9 Vacuum System and Electronics.

The vacuum chamber for the spectrometer was machined from lengths of aluminium alloy tubing, which were joined together using Varian Torrseal epoxy resin, which has an extremely low vapour pressure. Joints between the chamber and windows, etc., were made using Viton O-rings. Pumping was by a 2" liquid-nitrogen trapped oil diffusion pump and a 6" diameter titanium sublimation pump, giving a residual vacuum of approximately 1 10^{-7} Torr.

This was adequate to give stable field-ion emission from the refractory metals (W, Re, Rh, Mo). As explained above, it was originally intended that the vacuum system and analyser should be the prototype for a fully UHV stainless steel system. Although the second analyser was not built, for reasons of expense and time, the prototype analyser worked well, and a careful choice of experiments, keeping the vacuum limitations in mind, allowed useful data to be obtained.

Research grade gases were supplied dynamically to the vacuum chamber from glass flasks (BOC). The pressure in the analyser, when field-ion spectra were being recorded, was kept low ($< 5\ 10^{-6}$) so that the mean free path of the ions was large compared to the length of the flight-path to the detector.

The specimen high voltage was supplied from a Brandenburg α-series 30 KV generator, adjusted using a ten-turn helipot. The generator was calibrated using a Computing Techniques resistive voltage divider and a Fluke secondary standard differential voltmeter. The generator performed well up to its specified stability (40ppm/15 min) and no problems due to drift of the tip voltage were experienced.

The high-voltage supply to the energy analyser was derived from a VG Electronics type M5K2 5KV generator. The output of this unit can be set digitally to better than one volt; the stability and ripple performance of this supply were checked using the Fluke differential voltmeter and an oscilloscope, and were also found to be more than adequate.

The value of the current-limiting resistor between the Brandenburg generator and the specimen was adjusted according to the experiment in progress. For studying field-ion spectra a 25 MΩ resistor was used; it was found that if the more conventional

value of 1 GΩ was used a stable energy spectrum could not be readily attained, with fluctuations of a few volts being observed. This was not unexpected, as leakage currents of the order of 1 nA, which would produce such fluctuations, imply a resistance of approximately $10^{13}\Omega$ between the tip and ground potential. Reducing the limiting resistor to 25 MΩ reduced any instabilities to less than the resolution of the energy analyser. The limiting resistor was reduced to 10 KΩ during experiments in which negative pulses were applied to the screen, as will be described below.

2.6 Summary.

In the first part of this chapter a brief review of energy-analytical techniques in FIM showed how useful information on field-ionization and on the performance of the atom-probe can be obtained. Some areas of current interest, such as field-adsorption and plasmon losses, were mentioned. The severity of the experimental requirements of energy-analytical techniques in FIM were outlined, and a review of energy-analysers discussed the ability of various instruments to meet these requirements. An energy-analyser of potentially high sensitivity and resolution was selected, and its design and construction described in some detail. The use of a single micro-channel plate intensifier as a focal-plane detector, and in particular its ability to record single ions on film, were discussed.

The next chapter will describe the experimentally-determined performance of the energy analyser, and the operating procedures adopted; the use of the energy analyser in field-adsorption experiments will also be described. The energy analysis of field-evaporated ions will be discussed in Chapter 4.

Fig. 3.1

a) the focussed, and b) the unfocussed output from the detector, using the same monoenergergetic beam of helium ions. b) shows spurious peaks in the spectrum (see text). The energy scale is vertical, with the lowest energy at the top of the photographs.

a)

decreasing energy.

b)